Proc. Natl. Acad. Sci. USA
Vol. 87, pp. 2259–2263, March 1990
Cell Biology

Immunolocalization in three dimensions: Immunogold staining of cytoskeletal and nuclear matrix proteins in resinless electron microscopy sections

(embedment-free microscopy/colloidal gold)

JEFFREY A. NICKERSON, GABRIELA KROCKMALNIC, DACHENG HE, AND SHELDON PENMAN*

Department of Biology, Massachusetts Institute of Technology, Cambridge, MA 02139

Contributed by Sheldon Penman, December 14, 1989

ABSTRACT **We describe two methods for staining resinless thin sections with antibodies and gold-conjugated second antibodies. Immunolocalization of specific proteins is a powerful tool for cell structure studies but current techniques do not develop its full potential. Immunofluorescence provides only low-resolution localization, whereas conventional thin-section electron microscopy images and immunostains only the section surface. Resinless sections of extracted cell structures offer a simple and effective means of immuno-electron microscopy. Without embedding plastic or soluble proteins, the cell cytostructure produces high-contrast, three-dimensional images. Resinless sections of detergent-extracted cells are prepared by embedding in diethylene glycol distearate, sectioning, and removing diethylene glycol distearate before microscopy. In the first method of immunostaining, extracted cells were fixed and stained with antibodies before embedment, sectioning, removal of the embedding resin, and critical point drying. In the postembedment method, the sample was embedded and sectioned, the diethylene glycol distearate was removed, and the sample was rehydrated before antibody staining. With these techniques, specific proteins were localized with high resolution throughout the entire section. Stereoscopic micrographs of resinless sections revealed the precise localization of specific cytoskeleton and nuclear matrix proteins in three dimensions with unprecedented clarity.**

The localization of specific proteins with labeled antibodies is a fundamental technique for exploring cell structure. Cytoskeletal filaments were first displayed by immunofluorescent staining (1–4), profoundly changing our understanding of cell structure. Antibody-based localization achieves its highest resolution with the electron microscope. In the conventional technique samples are embedded in a resin that is cut into ultrathin sections. Antibodies stain the section surface wherever antigenic epitopes are exposed. An important advance in the conventional technology was the use of colloidal gold-conjugated second antibodies (5–7). This methodology is well suited for viewing cross sections of cell organelles and membrane systems. It is, however, severely limited for structures such as the cytoskeleton or nuclear matrix, whose form is apparent only when seen in three dimensions.

The conventional thin section is inadequate for imaging the structural networks of the cell, showing only that portion of the sample appearing at the section surface. This is because the embedding plastic presents the same average electron scattering cross section as biological materials and thus masks cellular components contained in the section interior. Heavy metals stain the section surface forming the actual image. Filaments of the structural networks are seen only in cross section unless, as rarely happens, they are tangent to the section surface. However, there is a simple and effective alternative to the embedded section. Cell structures form high-contrast, three-dimensional images without metal stains provided there is no embedding material (8, 9). Embedment-free samples can be prepared as cell whole mounts or as sections made using a temporary embedding medium (10, 11) that is removed before microscopy. The first embedment-free electron micrographs were difficult to interpret because of the dense mesh formed by fixed soluble proteins. However, these proteins are easily removed by detergent extraction prior to fixation. Using a temporary embedment medium, diethylene glycol distearate (DGD), ultrathin sections of cytoskeleton and nuclear matrix can be cut that are rigid and self supporting (11). After removal of the resin, these produce true three-dimensional images of cell structure that can be viewed stereoscopically. In such images the two distinct cellular filament networks, one in the cytoplasm and one in the nucleus, are seen to interconnect forming a cell framework or scaffold. These two networks join at the nuclear surface where the intermediate filaments and the nuclear matrix attach to the nuclear lamina (11, 12).

The utility of resinless sections would be enhanced by the ability to immunolocalize specific proteins in the imaged structures. In this report we describe two methods for accomplishing this. In the first method extracted cells were stained with monoclonal antibodies and gold bead-conjugated second antibodies prior to embedment and sectioning. In the second technique antibodies localized specific proteins after sectioning and rehydration. This second approach could be used to stain the same sample with several different antibodies, each antibody applied to a thin section. With these techniques, specific proteins could be localized with high resolution throughout the entire section. In the ideal application of this technique, stereoscopic micrographs of resinless sections showed the precise localization of specific proteins in three dimensions.

MATERIALS AND METHODS

Materials. Cells were grown on Mylar polyester film that was a kind gift from DuPont. The removable embedding resin DGD was obtained from Polysciences (no. 1873). Gold bead-conjugated goat anti-mouse IgG plus IgM was obtained from Janssen Life Sciences Products (no. 23.674.06). Anti-keratin monoclonal antibody was obtained from Boehringer Mannheim (no. AE1/AE3). The ascites form of 1B2 was the kind gift of Matritech (Cambridge, MA).

Cell Culture. HeLa cells (CCL 2) and MCF-7 cells (HTB 22) were grown in Dulbecco's medium with 7% and 10% fetal bovine serum, respectively. Rat aorta smooth muscle cells at

The publication costs of this article were defrayed in part by page charge payment. This article must therefore be hereby marked "*advertisement*" in accordance with 18 U.S.C. §1734 solely to indicate this fact.

Abbreviation: DGD, diethylene glycol distearate.

*To whom reprint requests should be addressed.

seventh passage were kindly supplied by Julie Inglefinger (Massachusetts General Hospital) and grown in Dulbecco's 10% fetal bovine serum. W12 cells were obtained from Margaret Stanley (University of Cambridge) and grown according to the methods of Stanley *et al.* (13). Trypsinized cells were plated onto sterile 1- to 2-cm^2 squares of Mylar in tissue culture dishes. Cells grown on Mylar were extracted and immunostained while still attached to their Mylar squares.

Cell Extractions. After a wash in phosphate-buffered saline (PBS), subconfluent cells were extracted for 3 min in cytoskeleton buffer [10 mM Pipes, pH 6.8/100 mM NaCl/300 mM sucrose/3 mM $MgCl_2$/1 mM EGTA/4 mM vanadyl riboside complex/1.2 mM phenylmethylsulfonyl fluoride/0.5% (vol/vol) Triton X-100] to remove soluble proteins. In some experiments this nucleus–cytoskeletal framework was extracted in RSB-magik [10 mM Tris·HCl, pH 7.4/10 mM NaCl/3 mM $MgCl_2$/4 mM vanadyl riboside complex/1.2 mM phenylmethylsulfonyl fluoride, 1% (vol/vol) Tween 40/0.5% (vol/vol) sodium deoxycholate] for 5 min. This stripped away the cytoskeleton leaving nuclei with their attached intermediate filaments. Chromatin was removed with 50–200 μg of RNase-free DNase I per ml (Boehringer Mannheim) at room temperature for 30 min in digestion buffer [10 mM Pipes, pH 6.8/50 mM NaCl/300 mM sucrose/3 mM $MgCl_2$/1 mM EGTA/4 mM vanadyl riboside complex/1.2 mM phenylmethylsulfonyl fluoride/0.5% (vol/vol) Triton X-100]. Ammonium sulfate was added from a 1 M stock solution to a final concentration of 0.25 M. This removed chromatin, leaving a nuclear matrix–intermediate filament structure, the RNA-containing nuclear matrix. Except for the DNase I digestion and 0.25 M ammonium sulfate elution, all steps are done at 4°C.

Preembedment Immunostaining. Following extraction, cells were fixed with freshly prepared 3.7% (wt/vol) paraformaldehyde in digestion buffer or 2.5% (vol/vol) glutaraldehyde in cytoskeleton buffer for 30 min at 4°C. Cells fixed in glutaraldehyde were incubated with 0.5 mg of $NaBH_4$ per ml in TBS-1 [10 mM Tris·HCl, pH 7.7/150 mM NaCl/3 mM KCl/1.5 mM $MgCl_2$/0.05% (vol/vol) Tween 20/0.1% (wt/vol) bovine serum albumin/0.2% (wt/vol) glycine] for 15 min at room temperature. After one rinse in digestion buffer, cells were washed twice for 5 min each at room temperature in TBS-1 and incubated in 5% (vol/vol) heat-inactivated normal goat serum in TBS-1 for 10 min at room temperature to block nonspecific binding. Incubation with the first antibody in TBS-1 with 1–5% heat-inactivated normal goat serum was at room temperature or 37°C for 1–2 hr or at 4°C overnight. Cells were washed three times for 5 min in TBS-1, blocked with 5% nonfat dry milk in TBS-1 for 10 min, and washed again three times in TBS-1 for 5 min. They were then blocked in 5% (vol/vol) heat-inactivated normal goat serum in TBS-1 for 5–10 min. Without rinsing they were incubated in gold-conjugated goat anti-mouse IgG plus IgM (5-nm diameter) diluted in TBS-2 [20 mM Tris·HCl, pH 8.2/140 mM NaCl/0.1% (wt/vol) bovine serum albumin] for 2 hr at room temperature. Cells were washed three times in TBS-1 for 10 min and two times in 0.1 M sodium cacodylate (pH 7.4) for 5 min before fixing for 30–60 min in 2.5% (vol/vol) glutaraldehyde in 0.1 M sodium cacodylate (pH 7.4). After three washes in the fixing buffer for 10 min each, cells were fixed in 2% osmium tetroxide in the same cacodylate buffer and dehydrated in steps culminating in three steps of 100% ethanol. The first 100% ethanol step contained freshly made eosin (saturated) to aid in the later localization of cells. Dehydrated samples were embedded, sectioned, and the embedding resin (DGD) was removed (11).

Samples were transferred from ethanol to butanol in a series of steps of increasing butanol concentration over 15 min before two changes of pure butanol for 5 min each. A third change of butanol was done at 60°C before a series of steps of increasing DGD concentration in butanol at 60°C to a final step of pure DGD. Samples were kept at 60°C in pure DGD for 2 hr with a change of DGD after 1 hr. Mylar squares were removed from the oven and placed on an aluminum foil with the sample side up. A drop of DGD at 60°C was placed on the squares and solidified as it cooled to room temperature. The Mylar was peeled off, the DGD-embedded cells were examined under an ultramicrotome microscope, and selected areas containing eosin-stained cells were cut out, mounted on empty DGD blocks, and sectioned. Sections were picked up on Formvar/carbon-coated copper grids. DGD was removed by immersing the sections in butanol at room temperature for 3–16 hr depending on the thickness of the section. In order to critical point dry the sections, they were transferred to ethanol with one intermediate step of butanol/ethanol (1:1). After two or three changes of pure ethanol the samples were critical point dried in a Tousimis Autosamdri (Rockville, MD) apparatus outfitted with filters to remove water and particulates from the liquid CO_2. The grids containing the dried samples were lightly carbon coated in a Kinney carbon evaporator and stored in a desiccator. Samples were examined using a JEOL 100C transmission electron microscope using an accelerating voltage of 80 kV.

Postembedment Immunostaining. In some experiments resinless sections were stained after embedment, sectioning, and removal of the embedding resin, DGD. Following extraction, cells were fixed with freshly prepared 3.7% paraformaldehyde in digestion buffer for 30 min at 4°C. They were dehydrated in a series of steps culminating in three steps of 100% ethanol. The first 100% ethanol step contained freshly made eosin (saturated) to aid in the later localization of cells. Dehydrated samples were embedded and sectioned, and the embedding resin (DGD) was removed (11).

Sections were rehydrated by steps from ethanol to TBS-1 and washed twice for 5 min each at room temperature in TBS-1. They were incubated in 5% (vol/vol) heat-inactivated normal goat serum in TBS-1 for 10 min at room temperature to block nonspecific binding. Incubation with the first antibody diluted in TBS-1 with 1–5% heat-inactivated normal goat serum was at room temperature or 37°C for 1–2 hr or at 4°C overnight. Cells were washed three times for 5 min in TBS-1, blocked with 5% nonfat dry milk in TBS-1 for 10 min, and washed again three times in TBS-1 for 5 min. They were then blocked in 5% (vol/vol) heat-inactivated normal goat serum in TBS-1 for 5–10 min. Without rinsing they were incubated in gold-conjugated goat anti-mouse IgG plus IgM (5-nm diameter) diluted in TBS-2 for 2 hr at room temperature. Cells were washed three times in TBS-1 for 10 min and twice in 0.1 M sodium cacodylate (pH 7.4) for 5 min before fixing for 30–60 min in 2.5% (vol/vol) glutaraldehyde in the same buffer. Samples were postfixed with 2% osmium tetroxide in the same buffer for 10 min before dehydration, critical point drying, and carbon coating.

RESULTS

We have developed two techniques for staining resinless sections with gold bead-conjugated antibodies. The electron micrographs presented here were made using the preembedment immunostaining technique, the technique yielding the best preservation of morphology. Samples were lightly fixed, incubated with the primary antibody, then incubated with a gold bead-coupled second antibody, and fixed again before embedding in the removable resin, DGD. In the second method antibody staining was performed after the sample was embedded, sectioned, and rehydrated. This postembedment method was more difficult, requiring very careful handling of delicate sections through the staining and wash steps, but in this way different sections from the same sample could be stained with different primary antibodies.

Cells were grown on Mylar polyester film, which simplified sample handling during staining and was easily removed after embedding. The cells were extracted with Triton X-100 before fixation to remove soluble proteins. When nuclear matrix structure was examined, the masking chromatin was removed with nuclease digestions and elevated salt concentrations. The preparation was then fixed with either glutaraldehyde or paraformaldehyde. After blocking with goat serum, the excess serum was removed and the extracted cell was incubated with an antibody against a cytoskeletal or nuclear matrix protein. The sample was then incubated with the gold bead-conjugated second antibody followed by washing and a second fixation with glutaraldehyde and osmium tetroxide. The sample was embedded in DGD, thin sections were cut and placed on Formvar-covered grids, and the embedding resin was removed before critical point drying and carbon coating. In the absence of embedding resin, the cell cytostructure formed high-contrast images without heavy metal stains. The gold beads appeared as opaque microspheres decorating the cytostructure.

Fig. 1 shows two examples of immunogold staining of cytoskeletal structures. Fig. 1*a* shows the immunostaining of detergent-extracted MCF-7 breast carcinoma cells with an anti-cytokeratin monoclonal antibody. Gold beads decorate the 10-nm keratin filaments shown in the region near the nucleus. No staining could be found in the nuclear space. Conventional electron microscopic images of keratin filaments show only short stretches where these are adjacent to the section surface. In contrast, resinless sections imaged the entire length of keratin filaments lying within the section volume. The keratins were anchored to the nuclear lamina and crossed the cytoplasmic space to the cell periphery. When resinless sections were viewed in stereo, cytoplasmic filament networks were seen in three dimensions filling the section volume. Such three-dimensional localization of structural proteins within the resinless section often provides a more complete and realistic picture of cell architecture.

Fig. 1*b* shows the staining with myosin antibodies of a structure difficult to see by conventional means (14), the smooth muscle cell cytoskeleton. Primary smooth muscle cells from rat aorta were cultured on Mylar, extracted with Triton X-100, fixed, and incubated with anti-myosin antibody. Myosin was highly localized in complexes that may correspond to the dense bodies of smooth muscle (15, 16).

Resinless section electron microscopy has been important for studies of nuclear matrix morphology (12). Optical microscopy cannot resolve the fine structure of the nuclear matrix and the conventional embedded thin-section images the nuclear matrix fibers poorly. Resinless sections show the matrix structure in three dimensions with great clarity. The nuclear matrix, seen in this way, is unlike any previously described subcellular organelle and is composed of polymorphic fibers with a complex, cell type-specific protein composition (17).

Fig. 2 shows two patterns of nuclear matrix protein localization. The nuclear matrix was revealed by removing the cytoskeleton and chromatin by the now well-characterized *in situ* fractionation procedure (12). This method was developed by determining the gentlest conditions that would remove enzyme-cleaved chromatin from the nucleus. A moderate concentration (0.25 M) of ammonium sulfate effectively removes all of the nucleosomes and most of the cytoskeleton but leaves the nuclear matrix structure intact (12).

Fig. 2*a Inset* shows the immunofluorescence staining pattern of one of these anti-nuclear matrix monoclonal antibodies, B2A10, in the nuclei of MCF-7 cells. The staining pattern, exclusively nuclear, is brightly speckled on a diffuse background with dark, unstained nucleoli, a typical nuclear matrix protein distribution. The resinless section electron micrograph shows the fine structure of the distribution of B2A10.

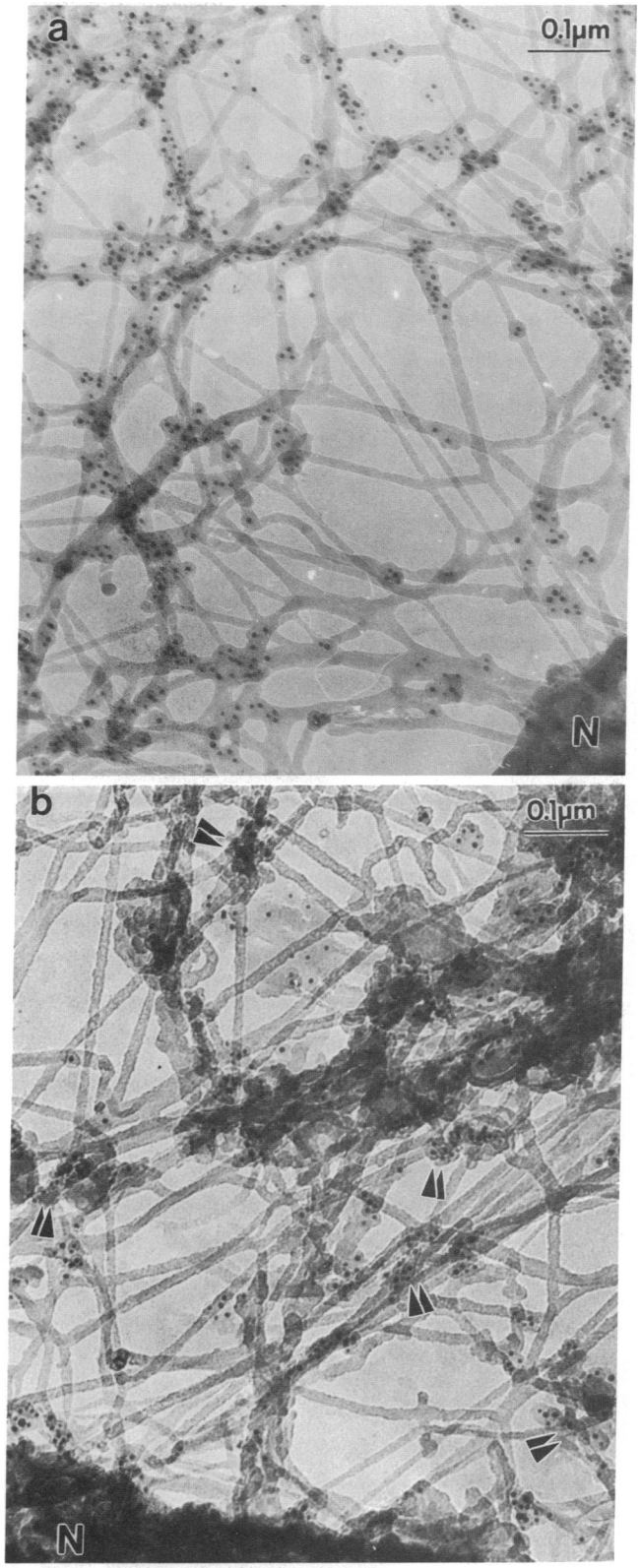

FIG. 1. Resinless section immunogold staining of the cytoskeleton. (*a*) Anti-cytokeratin staining of MCF-7 cells. Cells, grown on Mylar sheets, were extracted and stained with monoclonal anti-keratin antibody followed by gold bead-conjugated goat anti-mouse IgG before preparing resinless sections. N = nucleus. (*b*) Smooth muscle cells from rat aorta at seventh passage, grown on Mylar sheets, were stained with monoclonal anti-myosin and a gold bead-conjugated second antibody. N = nucleus; arrowheads indicate clusters of gold beads.

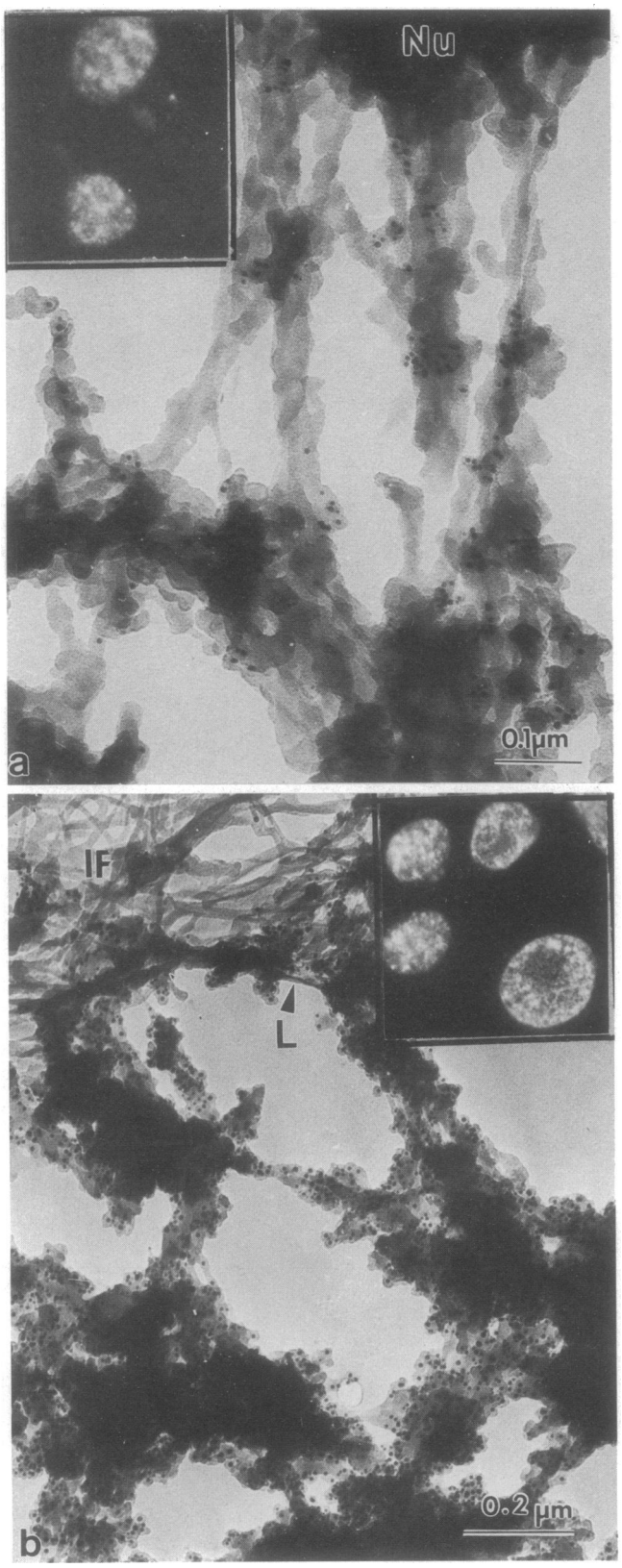

FIG. 2. Distribution of nuclear matrix proteins detected by resinless section immunogold staining. Cells were extracted, digested with DNase I, and salt extracted with 0.25 M ammonium sulfate to reveal the nuclear matrix. The cells were stained with monoclonal antibodies and then stained with either rhodamine-conjugated (*Insets*) or gold bead-conjugated second antibodies. (*a*) MCF-7 cells stained with the monoclonal antibody B2A10. Nu = residual nucleolus; arrowheads indicate clusters of gold beads. (*b*) W12 cervical cells stained with the H1B2 monoclonal antibody. L = nuclear lamina; IF = intermediate filaments.

The nuclear matrix preparation was stained with the B2A10 antibody and then with gold bead-conjugated second antibody and visualized by resinless section electron microscopy (Fig. 2*a*). The B2A10 antigen appeared in tight clusters mostly localized to knobs or swellings of the matrix fibers.

The monoclonal antibody H1B2 staining W12 cells from the human cervix (13) showed a very different distribution of nuclear matrix antigen. The immunofluorescence image seen in Fig. 2*b Inset* showed a speckled nuclear distribution. The immunogold resinless section microscopy revealed that H1B2 antibody densely decorated throughout the thick nuclear matrix fibers.

The structural changes in cells during mitosis are a challenging problem suitable for analysis by resinless section microscopy. In particular, the nuclear matrix-specific monoclonal antibodies can be used to see the disassembly, redistribution, and reassembly of the nuclear matrix during mitosis. Since chromatin is compacted into chromosomes from late prophase to early telophase, cells can be examined without the nuclease digestion necessary to uncover the nuclear matrix in interphase cells.

Fig. 3 shows, in both immunofluorescence and a stereoscopic electron microscopy pair, a mitotic HeLa cell extracted and stained with the H1B2 antibody. The distribution of the H1B2 antigen was surprising. Immunofluorescence surrounds the region of the chromosomes. The gold beads decorate 10-nm filaments radiating from the condensed chromosomes. These filaments, though similar in diameter, are not related to intermediate filaments that form a cage around the mitotic apparatus but more likely derive from the core filaments of the interphase nuclear matrix (18). These core filaments are revealed by a second elution of the interphase nuclear matrix with higher salt concentrations (18). Like the core filaments, these mitosis filaments were disrupted by RNase A (data not shown). The stereoscopic view best shows the three-dimensional architecture of the stained filaments.

The staining of resinless sections with colloidal gold-coupled antibodies could be done either before or after embedment. When HeLa cells were processed for postembedment staining (as described in *Materials and Methods*) and allowed to react with the H1B2 antibody after sectioning, removal of DGD, and rehydration, the resinless section image was essentially the same as that obtained by preembedment staining (data not shown), although in some cases the morphology was less well preserved.

DISCUSSION

In this report we present a powerful method for localizing structural proteins in the nuclear matrix and cytoskeleton of extracted cells. Monoclonal antibodies and colloidal gold-conjugated second antibodies were used to stain resinless sections of extracted cells. There are two important features of this technique. First, extraction of the cell before staining by a simple multistep *in situ* fractionation procedure removes all nonstructural proteins and, for staining the nuclear matrix, removes the chromatin (12). Taken to its final step, the extraction removes all protein structures except intermediate filaments, nuclear lamina, and interior nuclear matrix. The second feature, staining resinless sections rather than traditional embedded sections, permitted localization of proteins throughout the entire section and not just at the surface.

The pictures presented here were chosen to illustrate the method. However, they do illustrate important aspects of cell structure. The smooth muscle cytoskeleton has been difficult to visualize. The conventional embedded section shows little of the structure and so studies have employed immunofluorescence (19), immunostained frozen sections (19), freeze-etching (20), scanning microscopy of extracted cells (21), or isolation of cytoskeleton substructures (14, 16). These meth-

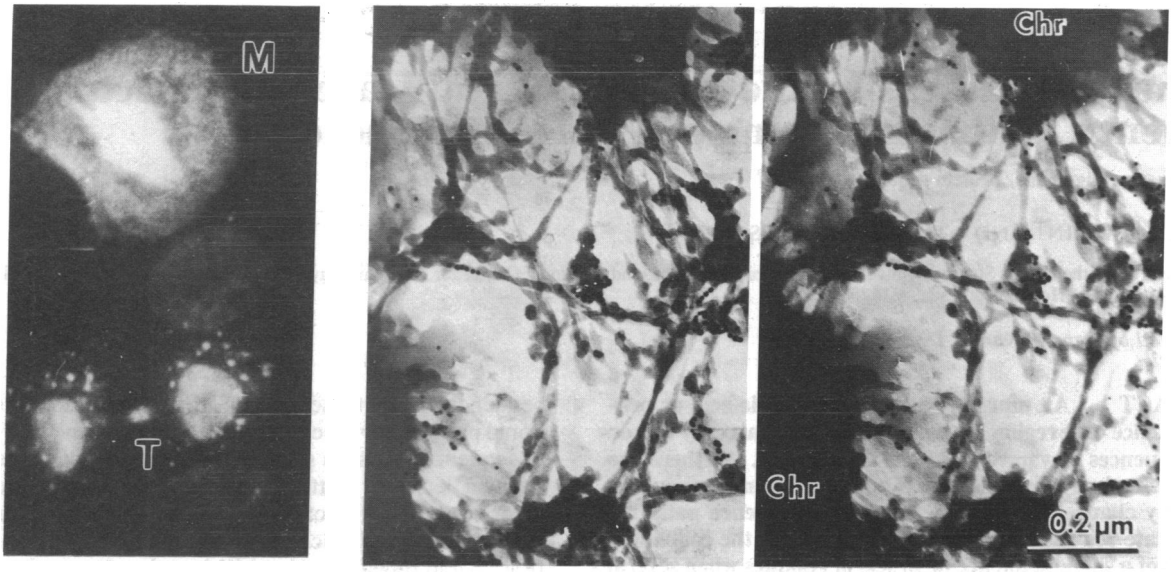

FIG. 3. Mitotic HeLa filaments decorated by H1B2 antibody. (*Left*) HeLa cells were synchronized by a double thymidine block. Synchronized cells on a glass slide were Triton X-100 extracted, fixed with paraformaldehyde, and stained with H1B2 and a rhodamine-conjugated second antibody. Phase images (not shown) show the fluorescent regions are localized to the vicinity of the chromosomes but do not appear to be associated with the mitotic spindle. Telophase cells also stain at the midbody. M = mitotic cell; T = posttelophase pair. (*Right*) A resinless section stereoscopic micrograph of a mitotic HeLa cell stained with H1B2 antibody. Cells were isolated by mitotic shake, extracted with Triton X-100, and processed in suspension. Cells were fixed with paraformaldehyde and stained with H1B2 and a gold bead-conjugated second antibody. The cells were embedded in DGD, sectioned, and processed. The micrographs were made at 10° total tilt angle. Chr = chromosome.

ods image very limited regions. Fig. 1*b* shows the smooth muscle cytoskeleton throughout the entire section. Myosin is localized in masses corresponding to the incompletely characterized dense bodies.

The distribution of nuclear matrix antigens was unforeseen. Fig. 2*a* is most typical and shows antigen in clusters throughout the matrix structure, often concentrated in lumps on the body of the nuclear matrix fibers. These fibers are heteromorphic in composition as well as in morphology and appear to be complex conglomerations of many different proteins (12, 17).

A different method of preparing and immunostaining extracted, resinless sections, particularly suitable for examining tissue ultrastructure, has been described by Katsuma *et al.* (22), who cut 10-μm sections from tissue that was rapidly frozen. Once thawed, the sections were sequentially extracted by procedures similar to those used here. Extracted liver sections were stained with monoclonal cytokeratin antibodies and gold bead-conjugated second antibodies. Because there was no embedding resin, gold beads could be easily seen decorating 10-nm intermediate filaments that stretched between the nuclear lamina and the cell periphery similar to those seen in Fig. 1. The frozen section technique is technically demanding compared to the resinless section technique, which is no more difficult than conventional embedding and sectioning. Further, unfixed frozen sections may be incapable of producing the very thin sections required for studies of the nuclear interior or dense cytoplasmic networks.

We thank Dr. Isobel Greenfield for the H1B2 immunofluorescence picture. This work was supported by National Institutes of Health Grants CA 08416 and CA 45480, National Science Foundation Grant DCB 8610388, and a grant from Whitaker Foundation.

1. Lazarides, E. & Weber, K. (1974) *Proc. Natl. Acad. Sci. USA* **71**, 2268–2272.
2. Lazarides, E. & Burridge, K. (1975) *Cell* **6**, 89–98.
3. Weber, K. (1976) in *Contractile Systems in Non-Muscle Tissues*, ed. Perry, S. V. (North-Holland, Amsterdam), pp. 51–66.
4. Goldman, R. D., Yerna, M. J. & Schloss, J. A. (1976) *J. Supramol. Struct.* **5**, 155–183.
5. Faulk, W. P. & Taylor, G. M. (1971) *Immunocytochemistry* **8**, 1081–1083.
6. Romano, E. L., Stolinski, C. & Hughes-Jones, N. C. (1974) *Immunocytochemistry* **11**, 521–522.
7. De May, J., Moeremans, M., Geuens, G., Nuydens, R. & De Brabander, M. (1981) *Cell Biol. Int. Rep.* **5**, 889–899.
8. Porter, K. R. (1984) *J. Cell Biol.* **99**, 3s–12s.
9. Wolosewick, J. J. & Porter, K. R. (1976) *J. Cell Biol.* **82**, 114–139.
10. Wolosewick, J. (1980) *J. Cell Biol.* **86**, 675–681.
11. Capco, D. G., Krochmalnic, G. & Penman, S. (1984) *J. Cell Biol.* **98**, 1878–1885.
12. Fey, E. G., Krochmalnic, G. & Penman, S. (1986) *J. Cell Biol.* **102**, 1654–1665.
13. Stanley, M. A., Browne, H. M., Appleby, M. & Minson, A. C. (1989) *Int. J. Cancer* **43**, 672–676.
14. Cooke, P. H., Kargacin, G., Craig, R., Fogarty, K. & Fay, F. S. (1987) *Prog. Clin. Biol. Res.* **245**, 1–25.
15. Bond, M. & Somlyo, A. V. (1982) *J. Cell Biol.* **95**, 403–413.
16. Tsukita, S., Tsukita, S. & Ishikawa, H. (1983) *Cell Tissue Res.* **229**, 233–242.
17. Fey, E. G. & Penman, S. (1989) *Proc. Natl. Acad. Sci. USA* **85**, 121–125.
18. He, D., Nickerson, J. A. & Penman, S. (1990) *J. Cell Biol.*, in press.
19. Geiger, B., Dutton, A. H., Tokuyasu, K. T. & Singer, S. J. (1981) *J. Cell Biol.* **91**, 614–628.
20. Somlyo, A. V. & Franzini-Armstrong, C. (1985) *Experientia* **41**, 841–856.
21. Ip, W. & Fischman, D. A. (1979) *J. Cell Biol.* **83**, 249–254.
22. Katsuma, Y., Marceau, N., Ohta, M. & French, S. W. (1988) *Hepatology (Baltimore)* **8**, 559–568.